ORIENTAL JOURNAL OF CHEMISTRY
An International Open Access, Peer Reviewed Research Journal
www.orientjchem.org
ISSN: 0970-020 X
CODEN: OJCHEG
2025, Vol. 41, No.(3):
Pg. 972-978

Study of Anticancer activity of Active form of vitamin D Analogs Against BRCA-1 and BRCA-2 based on Molecular docking and DFT Method

SABRINA HELEN[1]*, MUHAMMAD ABUL KASHEM LITON[1], ARABINA AKTER POTHI[2], MD. SHALAUDDIN[1] and MUKTA DAS[1]

[1]Department of Chemistry, Faculty of Science, Mawlana Bhashani Science and Technology University, Santosh, Tangail-1902, Bangladesh.
[2]Department of Obstetrics and Gynaecology, Dhaka Medical College Hospital, Dhaka-1000, Bangladesh.
*Corresponding author E-mail: sabrina01@mbstu.ac.bd

http://dx.doi.org/10.13005/ojc/410330

(Received: April 26, 2025; Accepted: June 09, 2025)

ABSTRACT

BRCA-1 and BRCA-2 is the breast cancer susceptible gene whose mutations cause genetic variation in DNA reparation proteins which ultimately increase the risk of cancer. Many epidemiological studies elicited that serum vitamin D concentration has strong association with immune system and confer a protective role against cancer cell growth and progression. 1α, 25-dihydroxyergocalciferol (L1) and 1α, 25-dihydroxycholecalciferol (L2) are the active form of vitamin D_2 and D_3. In the present study, molecular docking and quantum chemical computations through DFT were performed to investigate anticancer efficiency of 1α, 25-dihydroxyergocalciferol (L1) and 1α, 25-dihydroxycholecalciferol (L2) against BRCA-1(PDB ID: 5xst) and BRCA-2 (PDB ID: 5d2r) proteins. Our findings were compared with talazoparib, a reference drug. Blind docking revealed that both ligands show higher binding affinity for BRCA-1 (5xst) protein than talazoparib. Hence, we suggest that vitamin D may serve as a promising therapeutic candidate for the treatment of breast cancer.

Keywords: Breast cancer, 1α, 25-dihydroxyergocalciferol, 1α, 25-dihydroxycholecalciferol, DFT, Molecular docking.

INTRODUCTION

Breast cancer, one of the most appeared and progressive diagnosed malignant disease in woman all over the world. It is the second commencing reason of cancer related death among woman. The invaded rate of breast cancer is prevalent among woman aged 45-55 years[1]. 80%-woman age more than 50 years old and 40% woman within 65 years old are more susceptible to breast cancer[2–4]. Incidence of breast cancer turn doubled in 60/120 countries within 1990 and 2016 and mortality rate also become doubled in 43/102 countries[5]. Diverse internal and external factors are responsible for the development and incidence of breast cancer[6–8] like BRCA-1/2 mutations, hormonal influence, menopause, heredity, age, obesity, life style, oral contraceptives, vitamin D deficiency, environmental and social-psychological factors[9,10]. It has been reported that 5-10% breast

cancer can be stimulated due to genetic mutations and 20% to 30% of breast cancers are due to various modifiable factors[11].

Breast cancer gene BRCA-1 and BRCA-2 is tumor suppressor gene that play important role in fundamental cellular processes like chromatin reconstruction, transcription, cell cycle regulation and DNA repair processes[12]. They exhibit their tumor suppressor activity by interacting with numerous DNA reparation proteins[12–15]. More than 90% hereditary breast cancers are supposed to occur owing to BRCA-1/2 mutation[16]. Mutation in BRCA-1 and BRCA-2 proteins results development of reparation-deficient cell[14]. Hence cannot preserve genetic stability which incite uncontrolled breast epithelium cell proliferation and enhance the risk for breast cancer[14].

For breast cancer treatment diverse clinical methods are available including surgery, radiation, chemotherapy, hormone therapy and immunotherapy[17]. Several nutriment and vitamins are accessible that can inhibit the mutation of BRCA-1/2 protein by modifying and regulating chromatin structure and gene evolution. Several studies demonstrate that serum vitamin D concentration has converse interrelation with the incidence of breast cancer. Low extent of vitamin D in blood serum associated with provoked risk of various cancers including breast cancer. Contrarily, high extent of vitamin D in blood serum associated with reduced risk of various cancer growths[18].

Vitamin D is a fat-soluble steroidal hormone and micronutrient that exist in two forms: D_2 and D_3. The active form of vitamin D_2 is 1α, 25-dihydroxyergocalciferol which is emanated exogenously via diet and active form of vitamin D_3 is 1α, 25-dihydroxycholecalciferol which produced endogenously in skin followed by UV-B light absorption in the form of sun light[19,20]. Though calcium and phosphate homeostasis regulation is their main function[18], several *in vivo* and *in vitro* studies demonstrates that active form of vitamin D has significant inhibitory potency against breast cancer growth[21]. They exert their inhibitory potency via its nuclear receptor, vitamin D receptor (VDR). Upon ligand knotting, they not only activate diverse biological responses like chromatin structure, transcription of targeted gene but also, they flourish cell differentiation and inhibit specific cell proliferation[21].

In this study, we docked 1α, 25-dihydroxyergocalciferol and 1α, 25-dihydroxycholecalciferol against breast cancer receptor proteins BRCA-1 and BRCA-2. Then we investigate the interactions that occur between them and ascertain their binding affinity. After that obtained results were compared with a reference drug. For this, we take out targeted proteins BRCA-1 (5xst) and BRCA-2 (5d2r) from RCSB Protein Data Bank with most stable configuration. We also performed quantum chemical calculations through DFT. Within the framework of DFT, we analyzed dipole moment, frontier molecular orbitals, chemical reactivity descriptors and Mulliken atomic charges and then predict their sites of interaction, relative chemical reactivity and stability.

MATERIALS AND METHODS

All quantum mechanical calculations were performed using the Gaussian 09W software package[22]. The 3D structures of the studied ligands were constructed and visualized using Gauss View 6.0.16 software[23]. Geometry optimization of the studied ligands was accomplished in the framework of DFT by using B3LYP method and 6-311+G(2d,p) basis set[24-27]. After that, prepared ligands were imported into the PyRx AutoDock Vina Wizard[28] software for molecular docking. Docking simulations were performed to evaluate the binding affinity and to explore the interactions between ligands and targeted proteins BRCA-1 (5xst) and BRCA-2 (5d2r). During docking simulations, protein macromolecules were treated as rigid, while ligands were considered flexible with rotatable bonds.

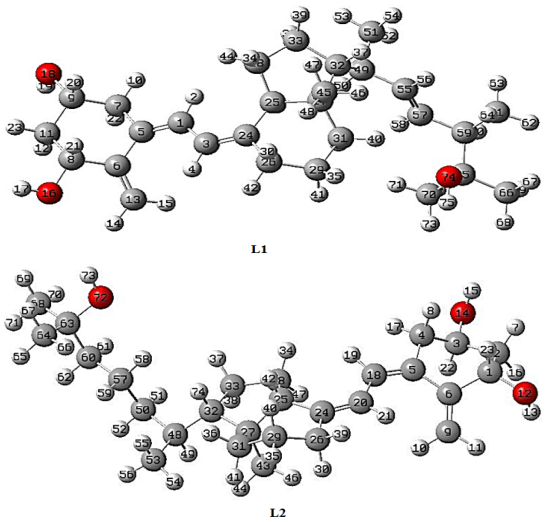

Fig. 1. Optimized structures of the studied ligands (L1 and L2). The color code for atoms: black for C, red for O and white for H

Preparation of Proteins

The X-ray crystallographic structures of breast cancer suppressor gene BRCA-1(5xst) and BRCA-2 (5d2r) were accessed from the RCSB Protein Data Bank at a structural resolution of 2.30 Å and 1.90 Å. To optimize the crystal structures and to ensure the crystal structures of the targeted proteins were in least energy Swiss-PDB viewer software package (version 4.1.0) was used[29]. All heteroatoms, water molecules and inhibitors of the proteins are removed and missing hydrogen's is added to the protein structures to construct the receptor for docking by using BIOVIA Discovery Studio Visualizer version 21.1.0.20298[30].

Molecular docking Studies

The docking analysis was performed using PyRx virtual screening tool in the protocol of Autodock Vina software. To execute docking proteins and ligands are taken into PDBQT format. Receptor grid box was place with such a measurement as it encircled the entire protein, where the centre was X: 28.6842, Y:-15.1989, Z:-20.2053 and the dimensions were X: 63.1249, Y: 54.2676 andZ: 71.8659 for BRCA-1 (PDB ID: 5xst). For BRCA-2 (PDB ID: 5d2r), the centre was X:-0.4808, Y: 32.2325, Z: 14.7683 and the dimensions were X: 61.2031, Y: 65.8440 and Z: 88.2615. The docking results were exposing as binding affinity energy and binding affinity energies were computed as negative scores in kcal/mol unit. The 2D and 3D binding pose of the docked protein-ligand complex were visualized by BIOVIA Discovery Studio Visualizer version 21.1.0.20298[30].

RESULTS AND DISCUSSION

Electric Dipole Moment

Density functional theory (DFT) is an efficient quantum mechanical framework for driving structure reactivity descriptors and to superintend the interactions immersed between the protein-ligand and drug-receptor[31]. The dipole moment is a crucial parameter that reflects the polarity of a molecule and the distribution of electronic charge. It influences molecular solubility, permeability, and potential interactions with proteins[32,33]. The calculated dipole moments of L1 and L2 (Table 1) suggest that both compounds possess considerable polarity, which may enhance their binding interactions with target proteins.

Frontier Molecular Orbitals and Chemical Reactivity Descriptors

The energies of HOMO and LUMO are important parameters for predicting the chemical reactivity of a compound. HOMO and LUMO energies were computed using DFT (B3LYP/6-311+G(2d,p)) and results are incorporated in Table 1. Ionization potential (I), electron affinity (A), chemical hardness (η), chemical softness (σ), electronegativity (χ), chemical potential (μ), electrophilicity index (ω) and maximum charge transfer index (ΔN_{max}) are the important chemical reactivity descriptors which assist to understand various aspects of chemical reactivity and kinetic stability of a compound. The energy of HOMO suggests the electron donating efficiency of a molecule while the energies of LUMO suggest the electron accepting competency of a molecule. These parameters can therefore help ascertain which molecular groups exhibit nucleophilic or electrophilic character. The HOMO–LUMO energy gap for both ligands is small, indicating higher chemical reactivity and polarizability. Ionization potential (I) and electron affinity (A) are very important two parameters from which we get information about how much energy is release or absorbed during electron transfer in a molecule. Both L1 and L2 show low ionization potential, suggesting that they require less energy for electron excitation, enhancing their potential to interact with target proteins. Negative chemical potential (μ) and small electrophilicity index (ω) of the studied ligands indicates that both ligands act as good nucleophile. The maximum charge transfer index (ΔN_{max}) for both ligands is also high, reflecting a strong tendency for electron uptake that may increase their binding affinity for the target proteins.

Table 1: Calculated total energy (joule), dipole moment (C.m) and chemical reactivity descriptors (joule) of the studied ligands (L1 and L2)

Parameters	L1	L2
Etotal	-5.752520×10^{-15}	-5.586466×10^{-15}
Dipole moment	6.6232×10^{-30}	1.1583×10^{-29}
EHOMO (J)	-8.97×10^{-19}	-7.28×10^{-19}
ELUMO (J)	-1.68×10^{-19}	-1.85×10^{-19}
Energy gap	7.28×10^{-19}	5.43×10^{-19}
Chemical reactivity descriptors		
Ionization potential (I)	8.97×10^{-19}	7.28×10^{-19}
Electron affinity (A)	1.68×10^{-19}	1.85×10^{-19}
Chemical hardness (η)	3.65×10^{-19}	2.72×10^{-19}
Chemical softness (σ)	1.82×10^{-19}	1.36×10^{-19}
Electronegativity (χ)	5.33×10^{-19}	4.56×10^{-19}
Chemical potential (μ)	-5.33×10^{-19}	-4.56×10^{-19}
Electrophilicity index (ω)	3.89×10^{-19}	3.82×10^{-19}
Maximum charge transfer index (ΔN_{max})	2.33×10^{-19}	2.67×10^{-19}

$I = -E_{HOMO}$, $A = -E_{LUMO}$, $\eta = (I - A)/2$, $\sigma = 1/2\ \eta$, $\chi = (I + A)/2$, $\mu = -(I + A)/2$, $\omega = \mu 2\ /2\ \eta$ and $\Delta N_{max} = -\mu/\eta$.

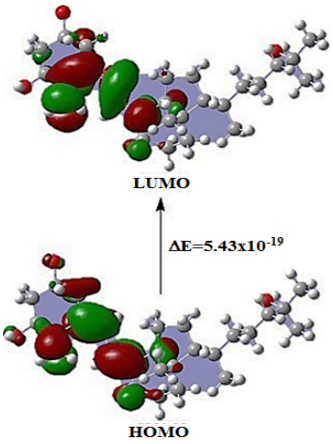

Fig. 2. HOMO-LUMO plots and energy gap for ligand L2 calculated at B3LYP/6-311+G(2d,p) level of DFT

Mulliken Atomic Charges

Mulliken atomic charge analysis was conducted to identify the most reactive atomic sites at the B3LYP/6-311+G (2d, p) level of DFT and obtained results are tabulated in Table A1 (shown in the supplemental material). For ligand L1 and L2, the highest positive charges were found at C65 and C63, indicating their susceptibility to nucleophilic attack, while the most negative charges at C29 and C60 suggest favorable sites for electrophilic interactions. These polar regions may influence the ligand's binding and biological activity.

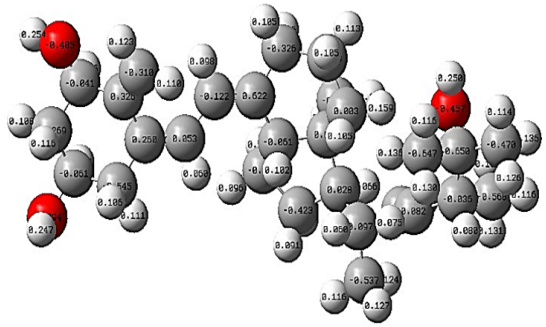

Fig. 3. Atomic charge distribution in ligand L1

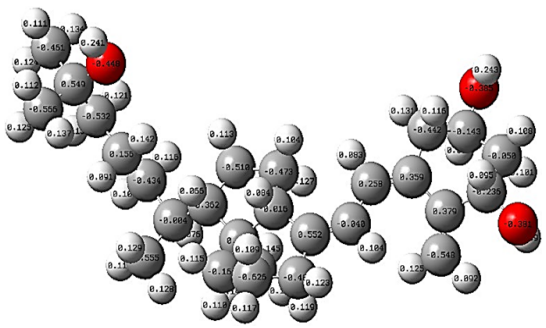

Fig. 4. Atomic charge distribution in ligand L2

Evaluation of Binding Affinity and Mode of Interactions of the Studied Ligands

We performed molecular docking simulations to score binding affinity and to explain the mode of interaction between the studied ligands and targeted proteins. Table 2 shows the binding affinity (kcal/mol) of our ligands against BRCA-1(5xst) and BRCA-2 (5d2r) receptor proteins. The ligands targeting 5xst and 5d2r receptor proteins showed binding affinities of -7.7 to -7.8 kcal/mol and -6.7 to -8.1 kcal/mol respectively. Both ligands exhibit strong hydrogen bond and hydrophobic interactions which promoted the nonbonding interactions and made it stable inside the cavity. We also docked a standard drug (talazoparib) against the targeted proteins and outcomes were compared to the investigated ligands. Relative to talazoparib, the studied ligands established more favorable interactions with 5xst amino acids and exhibited potent inhibition with binding affinities of –7.7 and –7.8 kcal/mol. Non-bonding interactions between the studied ligands and targeted proteins shown in Fig. 5. L2 exhibited the strongest binding affinity -7.8 kcal/mol for BRCA-1 and -8.1 kcal/mol for BRCA-2, outperforming the reference drug talazoparib. When L2 ligand is docked with 5d2r, it forms hydrogen bond between the hydrogen of hydroxyl group and oxygen of LYS269, the hydrogen of hydroxyl group and oxygen of GLY362. It also exhibits some hydrophobic interactions with PRO282 and VAL 364 which assist to strengthening its affinity for the corresponding protein. Ligand L2 also make stable complex with 5xst protein by forming two hydrogen bonds with ARG217, four hydrophobic interactions with LYS42, PRO220, LEU108, and VAL112. Ligand L1 form complex with 5xst and 5d2r proteins and possess significant binding affinity with a docking score of -7.7 and -6.7 kcal/mol. The hydrogen bonding and hydrophobic interactions between the ligands and proteins are depicted in Fig. B1 (shown in the supplemental material). The findings of blind docking studies demonstrated that the above-mentioned ligands form stable complex with the targeted proteins and may cause significant resistibility against cancer cell and cancer progression.

Table 2: Docking results of the studied ligands and reference ligand against BRCA-1(5xst) and BRCA-2 (5d2r) proteins

	BRCA-1(5xst)			BRCA-2 (5d2r)		
Ligands	Binding affinity energy (kcal/mol)	Hydrogen bonds	Hydrophobic interaction with residues	Binding affinity energy (kcal/mol)	Hydrogen bonds	Hydrophobic interaction with residues
L1	-7.7	A:ARG217:HN···O:UNK1:N(2.33649) N:UNK1:H···OD2:ASP105:A(2.73861)	A:LEU108-N:UNK1(4.03362)	-6.7	A:VAL364:HN···O:UNK1:N (1.97857) N:UNK1:H···O:VAL364:A (2.59699)	A:LYS280 - N:UNK1(5.47511) A:PRO282 - N:UNK1(4.77641)
L2	-7.8	A:ARG217:HN···O:UNK1:N(2.28436) N:UNK1:H···O:ARG217:A(2.36075)	A:LYS42-N:UNK1(4.51738) A:LEU108-N:UNK1(5.41316) A:VAL112-N:UNK1(5.39433) A:PRO220-N:UNK1(5.03229)	-8.1	N:UNK1:H···O:GLY362:A (2.24056) N:UNK1:H···O:LYS269:A (2.27319)	A:PRO282-N:UNK1(3.78563) A:VAL364 - N:UNK1 (4.388)
Talazoparib	-7.5	A:HIS161:HD1···N:UNK1:O(2.24739)	N:UNK1-A:LYS158(4.43363) N:UNK1-A:LYS158(3.91411) N:UNK1-A:LYS158(3.7077)	-8.1	A:GLY385:HN···N:UNK1:F(2.95396) A:SER387:HG···N:UNK1:H···A:GLU391:O(1.93717) A:ASN382:HD21···N:UNK1 (3.02661) A:ASN382:HD21···N:UNK1(2.98033) N:UNK1:H···A:HIS292(3.12935)	A:PHE337-N:UNK1 (4.76492) N:UNK1-A: PRO 394(4.80583) N:UNK1-A: ILE 384(5.18524)

Ligands	BRCA-1(5xst) Docked conformation	2D interaction diagrams between amino acid residue and ligand	BRCA-2 (5d2r) Docked conformation	2D interaction diagrams between amino acid residue and ligand
L1	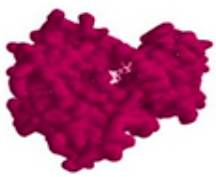	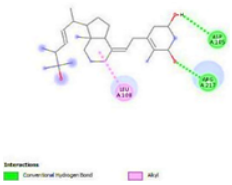	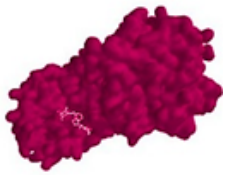	
L2	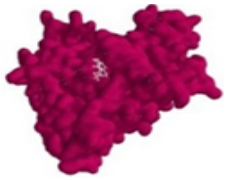	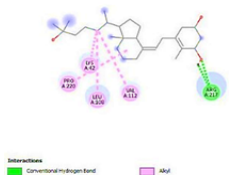	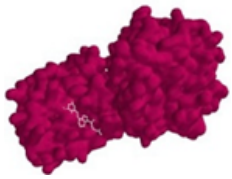	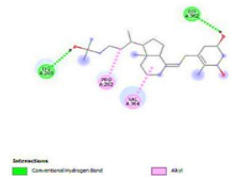
Talazoparib	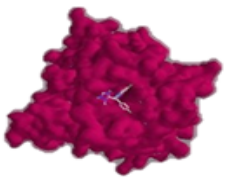	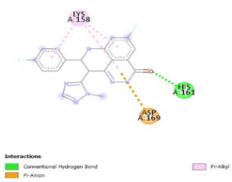	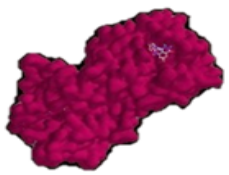	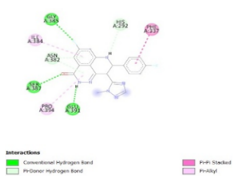

Fig. 5. Visualization of docked conformation at the active site of BRCA-1 (5xst) and BRCA-2 (5d2r) proteins and their 2D interactions

CONCLUSION

In this study, we employed molecular docking and DFT-based analysis to investigate the anticancer potential of vitamin D analogues (L1 and L2) against BRCA-1 and BRCA-2 proteins. To get information about relative chemical reactivity and stability of ligands L1 and L2, we investigate dipole moment, frontier molecular orbitals, chemical reactivity descriptors and Mulliken atomic charges in the framework of DFT utilizing B3LYP method with 6-311+G(2d,p) basis set. The data attained from molecular docking study are compared with the FDA approved drug talazoparib. Our findings suggest that both ligands exhibit favorable electronic properties and strong binding interactions, particularly L2. These results indicate the potential of these compounds as anticancer agents, though further experimental validation is necessary.

ACKNOWLEDGEMENT

The authors are greatly privileged to thank the Synthetic and Computational Chemistry Research Group, Department of Chemistry, Mawlana Bhashani Science and Technology University for their steerage and the scope provided to perform the research.

Conflict of interest

The authors report no conflict of interest regarding this publication.

REFERENCES

1. Jemal, A.; Siegel, R.; Ward, E.; Hao, Y.; Xu, J.; Thun, M. J., *CA Cancer J. Clin.*, **2009**, *59*(4), 225–249. https://doi.org/10.3322/caac.20006.
2. Benz, C. C., *Crit. Rev. Oncol. Hematol.*, **2008**, *66*(1), 65–74. https://doi.org/10.1016/j.critrevonc.2007.09.001.
3. Siegel, R.; Ma, J.; Zou, Z.; Jemal, A., *CA Cancer J. Clin.*, **2014**, *64*(1), 9–29.https://doi.org/10.3322/caac.21208.
4. McGuire, A.; Brown, J. A. L.; Malone, C.; McLaughlin, R.; Kerin, M., *J. Cancers (Basel).*, **2015**, *7*(2), 908–929.https://doi.org/10.3390/cancers7020815.
5. Sharma, R., *Breast Cancer.*, **2019**, *26*(4), 428–445.https://doi.org/10.1007/s12282-018-00941-4.
6. Obeagu, E. I.; Babar, Q.; Vincent, C. C. N.; Udenze, C. L.; Eze, R.; Okafor, C. J.; Ifionu, B. I.; Amaeze, A. A.; Amaeze, F. N., *J. Pharm. Res. Int.*, **2021**, 82–99.https://doi.org/10.9734/jpri/2021/v33i56a33889.
7. Aizaz, M.; Khan, M.; Khan, F. I.; Munir, A.; Ahmad, S.; Obeagu, E. I., *Int. J. Innov. Appl. Res.*, **2023**, *11*, 31–37.https://doi.org/10.58538/IJIAR/2008.
8. Ibekwe, A. M.; Obeagu, E. I.; Ibekwe, C. E.; Onyekwuo, C.; Ibekwe, C. V.; Okoro, A. D.; Ifezue, C. B., *J. Pharm. Res. Int.*, **2022**, 1–10.https://doi.org/10.9734/jpri/2022/v34i46a36371.
9. Obeagu, E. I.; Obeagu, G. U., *Med.*, **2024**, *103*(3), E36905.https://doi.org/10.1097/MD.0000000000036905.
10. Key, T. J.; Verkasalo, P. K., *Lancet Oncol.*, **2001**, *2*(3), 133–140. https://doi.org/10.1016/S1470-2045(00)00254-0.
11. Sun, Y. S.; Zhao, Z.; Yang, Z. N.; Xu, F.; Lu, H. J.; Zhu, Z. Y.; Shi, W.; Jiang, J.; Yao, P. P.; Zhu, H. P., *Int. J. Biol. Sci.*, **2017**, *13*(11), 1387–1397.https://doi.org/10.7150/ijbs.21635.
12. Orban, T. I.; Olah, E., *J. Clin. Pathol. -Mol. Pathol.*, **2003**, *56*(4), 191–197.https://doi.org/10.1136/mp.56.4.191.
13. Kerr, P.; Ashworth, A., *Curr. Biol.*, **2001**, *11*(16).https://doi.org/10.1016/S0960-9822(01)00389-X.
14. Welcsh, P. L.; King, M. C. Hum., *Mol. Genet.*, **2001**, *10*(7), 705–713.https://doi.org/10.1093/hmg/10.7.705.
15. Stecklein, S. R.; Jensen, R. A.; Pal, A., *Front. Biosci. -Elit.*, **2012**, *4E*(3), 934–949.https://doi.org/10.2741/e431.
16. Ford, D.; Easton, D. F.; Stratton, M.; Narod, S.; Goldgar, D.; Devilee, P., *Am. J. Hum. Genet.*, **1998**, *62*(3), 676–689.https://doi.org/10.1086/301749.
17. Fu, X.; Tan, W.; Song, Q.; Pei, H.; Li*, J. Front. Cell Dev. Biol.*, **2022**, *10*.https://doi.org/10.3389/fcell.2022.813457.
18. Feldman, D.; Krishnan, A. V.; Swami, S.; Giovannucci, E.; Feldman, B., *J. Nat. Rev. Cancer.,* **2014**, *14*(5), 342–357.https://doi.org/10.1038/nrc3691.
19. Jones, G.; Prosser, D. E.; Kaufmann, M., *J. Lipid Res.*, **2014**, *55*(1), 13–31.https://doi.org/10.1194/jlr.R031534.

20. Dogra, A. K.; Prakash, A.; Gupta, S.; Gupta, M.; Bhat, S. A., *Adv. Biomark. Sci. Technol.*, **2022**, *4*, 1–11.https://doi.org/10.1016/j.abst.2022.01.001.
21. Pickholtz, I.; Saadyan, S.; Keshet, G. I.; Wang, V. S.; Cohen, R.; Bouwman, P., *Oncotarget.,* **2014**, *5*(23), 11827–11846.https://doi.org/10.18632/oncotarget.2582.
22. Cheeseman, G. A. P. J.R.; Scalmani, G.; Barone, V.; Mennucci. B. Gaussian 09, Revision E.01. Gaussian, Inc., Wallingford Ct **2009**.
23. K, T. A.; Dennington, J. M. M. R. GaussView, Version 6. Semichem Inc., Shawnee Mission. KS **2016**.
24. Lee, C.; Yang, W.; Parr, R. G., *Phys. Rev*. B **1988**, *37*(2), 785–789. https://doi.org/10.1103/PhysRevB.37.785.
25. Becke, A. D., *J. Chem. Phys.*, **1993**, *98*(7), 5648–5652. https://doi.org/10.1063/1.464913.
26. Vural, H.; Uçar., *J. Coord. Chem.*, **2016**, *69*(20), 3010–3020. https://doi.org/10.1080/00958972.2016.1225042.
27. Azhagiri, S.; Jayakumar, S.; Gunasekaran, S.; Srinivasan, S. Spectrochim. *Acta-Part A Mol. Biomol. Spectrosc.*, **2014**, *124*, 199–202. https://doi.org/10.1016/j.saa.2013.12.106.
28. Trott, O.; Olson, A. J., *J. Comput. Chem.*, **2010**, *31*(2), 455–461.https://doi.org/10.1002/jcc.21334.
29. Guex, N.; Peitsch, M. C., *Electrophoresis.,* **1997**, *18*(15), 2714–2723. https://doi.org/10.1002/elps.1150181505.
30. Abuzinadah, M. F.; Ahmad, V.; Al-Thawdi, S.; Zakai, S. A.; Jamal, Q. M. S., *Nutrients.,* **2022**, *14*(15).https://doi.org/10.3390/nu14153045.
31. Jordaan, M. A.; Ebenezer, O.; Damoyi, N.; Shapi, M., *Heliyon.*, **2020**, *6*(8).https://doi.org/10.1016/j.heliyon.2020.e04642.
32. Eroglu, E.; Türkmen, H., *J. Mol. Graph. Model.*, **2007**, *26*(4), 701–708.https://doi.org/10.1016/j.jmgm.2007.03.015.
33. Semeniuk, A.; Kalinowska-Tluscik, J.; Nitek, W.; Oleksyn, B. J., *J. Chem. Crystallogr.*, **2008**, *38*(5), 333–338. https://doi.org/10.1007/s10870-008-9327-9.